A Compact and Low-Profile Loop Antenna With Six Resonant Modes for LTE Smartphone

Hang Xu, Hanyang Wang, *Senior Member, IEEE*, Steven Gao, *Member, IEEE*, Hai Zhou, Yi Huang, *Senior Member, IEEE*, Qian Xu, and Yujian Cheng, *Senior Member, IEEE*

***Abstract*— In this paper, a novel six-mode loop antenna covering 660–1100, 1710–3020, 3370–3900, and 5150–5850 MHz has been proposed for the application of long-term evolution (LTE) including the coming LTE in unlicensed spectrum and LTE-Licensed Assisted Access. Loop antennas offer better user experience than conventional planar inverted-F antennas (PIFAs), inverted-F antennas (IFAs), and monopole antennas because of their unique balanced modes (1λ, 2λ, . . .). However, the bandwidth of loop antennas is usually narrower than that of PIFA/IFA and monopole antennas due to these balanced modes. To overcome this problem, a novel monopole/dipole parasitic element, which operates at an unbalanced monopole-like 0.25λ mode and a balanced dipole-like 0.5λ mode, is first proposed for loop antennas to cover more frequency bands. Benefiting from the balanced mode, the proposed parasitic element is promising to provide better user experience than conventional parasitic elements. To the best of the authors' knowledge, the balanced mode for a parasitic element is reported for the first time. The proposed antenna is able to provide excellent user experience while solving the problem of limited bandwidth in loop antennas. To validate the concept, one prototype antenna with a size of 75 × 10 × 5 mm^3 is designed, fabricated, and measured. Both simulations and experimental results are presented and discussed. Good performance is achieved.**

***Index Terms*— Handset antennas, long-term evolution (LTE) antenna, loop antennas, LTE-Licensed Assisted Access (LTE-LAA), LTE-unlicensed (LTE-U), mobile antennas, multiband antenna, parasitic element.**

I. Introduction

ULTRATHIN smartphones have become essential devices in people's daily life due to their powerful functionality such as navigation, entertainment, social networking service, and mobile financial service. Loop antennas have received extensive attention for long-term evolution (LTE) smartphones due to their unique features such as multimode and balanced modes (1λ, $2\lambda, \ldots$) [1]–[12]. The balanced modes have much weaker surface current distribution on printed circuit board (PCB) than the unbalanced modes that are the common operating modes of planar inverted-F antennas (PIFAs), inverted-F antennas (IFAs), and monopole antennas [13]–[18]. This property can give loop antennas better user interaction robustness and smaller antenna performance degradation than conventional PIFAs/IFAs and monopole antennas when a mobile phone is held by a user's hand or attached to a user's head [19]–[21]. This is important for user experience in smartphone application.

However, weaker surface current distribution on PCB also means less effective radiation area for loop antennas. As a result, the bandwidth of loop antennas is usually narrower than that of conventional PIFAs/IFAs and monopole antennas. To overcome the problem of limited bandwidth, there has been lots of research work on loop antennas for mobile phones. Nevertheless, the loop antennas in [1], [5], and [20] can excite only three resonant modes including 0.5λ, 1λ, and 1.5λ modes, which limits their bandwidth. In [11] and [12], reconfigurable technology was applied in loop antenna, but the covered bandwidth is still limited. Recently, the fourth mode, i.e., 2λ mode, was reported in [4] and [7] to cover wider frequency band (698–960 and 1710–2300 MHz in [4]; 800–1100 and 1700–2580 MHz in [7]), but the bandwidth is still not wide enough for LTE application and even the coming LTE in unlicensed spectrum (LTE-U) and LTE-Licensed Assisted Access (LTE-LAA) application [22], [23]. Therefore, although many scientists have made a lot of efforts, it is still a tremendous challenge for loop antennas to enjoy the excellent user experience while obtaining a bandwidth wide enough for LTE smartphone application.

In this paper, a novel six-mode loop antenna covering 660–1100, 1710–3020, 3370–3900, and 5150–5850 MHz is proposed for LTE smartphones. The bandwidth of the proposed antenna is wide enough for almost all the service of mobile telecommunication systems, namely, GSM/UMTS/LTE, including LTE bands 42/43 (3400–3800 MHz) and LTE-U/LTE-LAA (5150–5850 MHz) as well. The distinctive feature of the proposed antenna is that not only four loop antenna modes, i.e., 0.5λ, 1λ, 1.5λ, and 2λ modes, have been excited, but also two extra modes are generated by a proposed monopole/dipole parasitic element, i.e., an unbal-

Manuscript received January 2, 2016; revised March 13, 2016; accepted April 23, 2016. Date of publication June 27, 2016; date of current version September 1, 2016. This work was supported by Huawei Technologies Company, Ltd., China.

H. Xu and S. Gao are with the School of Engineering and Digital Arts, University of Kent, Canterbury CT2 7NT, U.K. (e-mail: hx21@kent.ac.uk; s.gao@kent.ac.uk).

H. Wang and H. Zhou are with Huawei Technologies Company, Ltd., Reading RG2 6UF, U.K. (e-mail: hanyang.wang@huawei.com; hai.zhou1@huawei.com).

Y. Huang and Q. Xu are with the Department of Electrical Engineering and Electronics, University of Liverpool, Liverpool L69 3GJ, U.K. (e-mail: yi.huang@liverpool.ac.uk; qian.xu@liverpool.ac.uk).

Y. Cheng is with the EHF Key Laboratory of Fundamental Science, School of Electronic Engineering, University of Electronic Science and Technology of China, Chengdu 611731, China (e-mail: chengyujian@uestc.edu.cn).

Color versions of one or more of the figures in this paper are available online at http://ieeexplore.ieee.org.

Digital Object Identifier 10.1109/TAP.2016.2582919

anced monopole-like 0.25λ mode and a balanced dipole-like 0.5λ mode. Usually, a parasitic element operates at an unbalanced monopole-like 0.25λ mode and/or an unbalanced 0.75λ mode but not a balanced dipole-like 0.5λ mode, so it should be the first time to report that a parasitic element could operate at a balanced dipole-like 0.5λ mode. Benefiting from the wideband feature and the three balanced modes, the proposed antenna is able to provide excellent user experience while solving the problem of limited bandwidth in loop antennas. The proposed antenna has been simulated, fabricated, and measured. All the simulated results were obtained using Ansoft HFSS [24]. The measured reflection coefficient and radiation efficiency were obtained using a Rohde and Schwarz vector network analyzer and a reverberation chamber, respectively [25]–[27].

II. Methodology, Analysis, and Discussion of Bandwidth Enhancement Technology

In order to explain the concept of the proposed antenna clearly, this section starts from the design of one four-mode loop antenna with enhanced bandwidth in Section II-A. In Section II-B, a single-mode parasitic element is introduced at first and then further developed to a monopole/dipole parasitic element to cover LTE bands 42/43 and LTE-U/LTE-LAA. In-depth analysis and discussions about radiation mechanisms are presented in Section II-C. In Section II-D, some design guidance is given.

A. Bandwidth Enhancement for Loop Antenna Modes

In this section, a four-mode loop antenna that can cover 680–1000 and 1665–2765 MHz is proposed as a starting point.

1) Antenna Configuration: The configuration of the proposed four-mode loop antenna is shown in Fig. 1. It is designed on a single-sided PCB ($\varepsilon r = 4.4$ and loss tangent $= 0.02$) with a dimension of $145 \times 75 \times 1.6$ mm^3. The antenna is placed on a 5-mm-high foam carrier ($\varepsilon r = 1$), which is located at the bottom edge of the PCB, as shown in Fig. 1(a). There is a 10-mm ground plane clearance below the antenna, so the total antenna volume is $75 \times 10 \times 5$ mm^3.

The loop antenna has two connections to the PCB. One is a feeding point, and the other is a grounding point as shown in Fig. 1(b) and (c). Most parts of the antenna have an identical width of 1 mm except two loading/deloading parts [28]. In Fig. 1(c), detailed dimensions of the antenna are shown and the dashed line is for bending the antenna track. The coplanar waveguide portion on the PCB is used for a matching circuit to enhance the bandwidth of 0.5λ mode.

2) Bandwidth Comparison and Analysis: Simulated $S11$ of the antenna in Fig. 1 is shown in Fig. 2. In low band, the -6 dB impedance bandwidth can cover 833–973 MHz, and then it can be further enhanced by a high-pass matching circuit to cover 680–1000 MHz (the high-pass matching circuit will be shown in Section IV). In high band, the -6 dB impedance bandwidth can cover 1665–2765 MHz, which is wider than the four-mode loop antennas in [4] (1710–2300 MHz) and [7] (1700–2580 MHz).

One important issue of the proposed design is the use of a widened portion A (shown in Fig. 1), which has

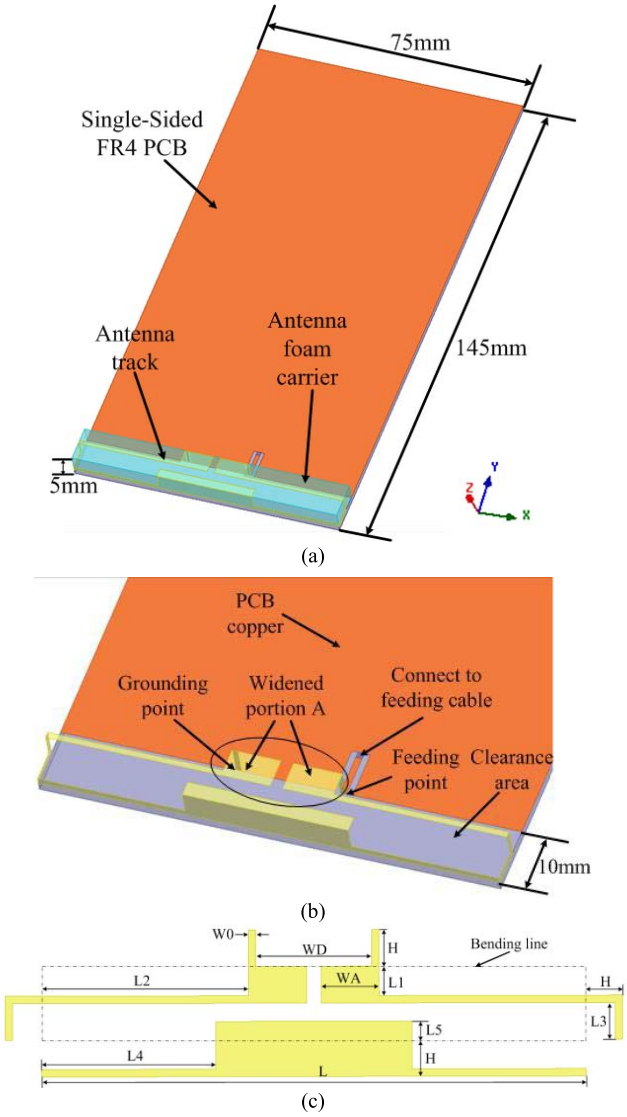

Fig. 1. Geometry of a four-mode loop antenna. (a) Antenna with PCB. (b) Antenna track. (c) Dimension of the antenna track. WD $= 16$, $W0 = 1$, $H = 5$, WA $= 8$, $L1 = 4$, $L2 = 28.5$, $L3 = 5$, $L4 = 24$, and $L5 = 2.5$ mm.

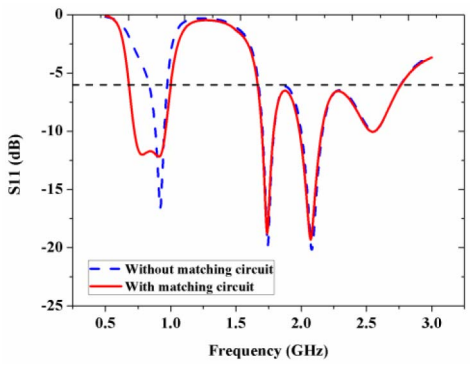

Fig. 2. Simulated $S11$ of the proposed four-mode loop antenna.

significant effect on the bandwidth enhancement of 1λ, 1.5λ, and 2λ modes. In order to explain the principle of the bandwidth enhancement, vector current distribution of 1.5λ mode is plotted in Fig. 3 for three antennas including

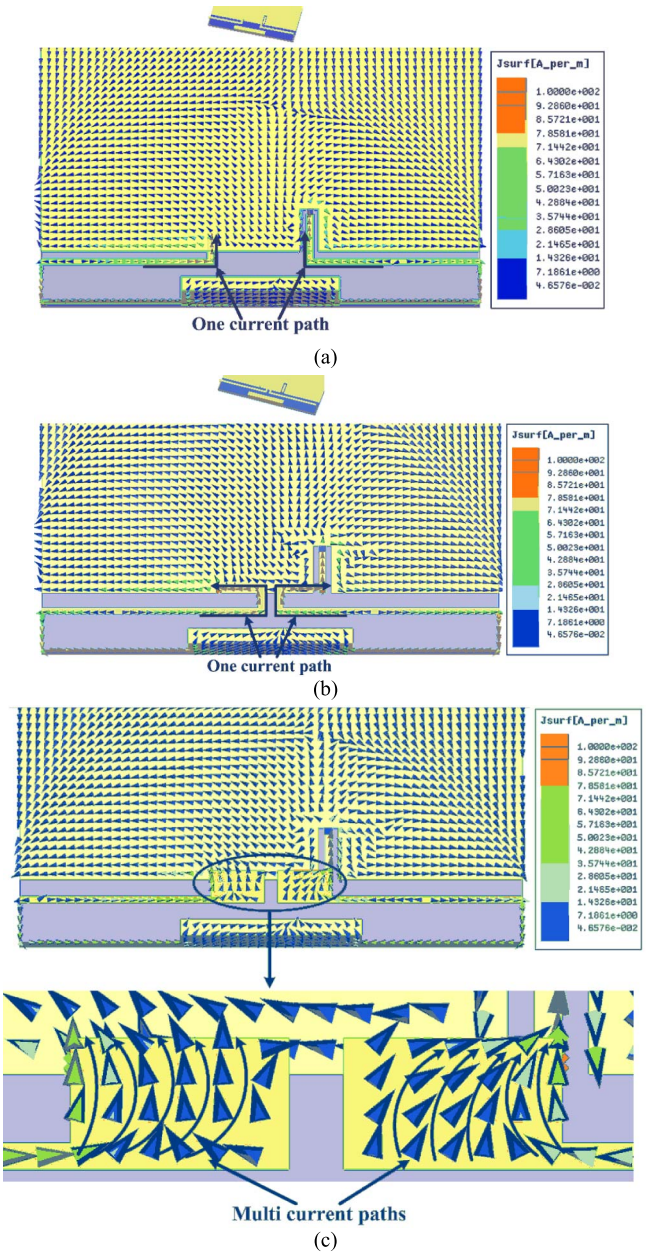

Fig. 3. Vector current distribution. (a) Ref-1. (b) Ref-2. (c) Proposed loop antenna.

two reference antennas (Ref-1 and Ref-2) and the proposed loop antenna. Except the widened portion A, the rest parts of reference antennas are the same as the proposed antenna. From Fig. 3(a) and (b), it can be seen that there is only one current path along the antenna track. From Fig. 3(c), it is clearly shown that there are multiple current paths in the widened portion A and different current paths have different electrical lengths, which means that the combination of different current paths can have wider bandwidth. This is how the bandwidth is enhanced by the widened portion A.

To demonstrate our analysis, simulated $S11$ of the three antennas is shown in Fig. 4. As predicted, for the 1λ mode, the relative bandwidth increases from 7.2% (Ref-1) and 6.8% (Ref-2) to 10.4% (the proposed antenna). For the 1.5λ mode, the relative bandwidth increases from 7.6% (Ref-1) and 8.6% (Ref-2) to 21.3% (the proposed antenna).

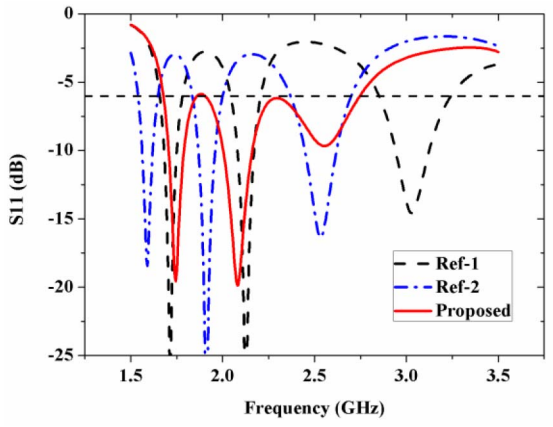

Fig. 4. Simulated $S11$ of Ref-1, Ref-2, and the proposed loop antennas.

For the 2λ mode, the relative bandwidth increases from 12.8% (Ref-1) and 13.1% (Ref-2) to 17.5% (the proposed antenna). As a result, the total relative bandwidth of 1λ, 1.5λ, and 2λ modes increases from 27.6% (Ref-1) and 28.5% (Ref-2) to 49.2% (the proposed antenna) because of the widened portion A.

However, this bandwidth enhancement technique has little effect on the bandwidth of 0.5λ mode. The reason is that in the frequency range below 1 GHz, PCB contributes most of the radiation rather than the antenna [29], so the improvement of the current path on the antenna track has limited effect on the bandwidth.

B. Evolution of Parasitic Element Technology

According to the result in Section II-A, 680–1000 and 1665–2765 MHz can be fully covered using one loop antenna. Nevertheless, the bandwidth is still not wide enough to meet the requirement of mobile telecommunication service, but the bandwidth of four-mode loop antennas has come to the extremity. In this section, parasitic element technology is introduced and further developed to cover more frequency bands.

1) Single-Mode Parasitic Element: At first, a single-mode parasitic element is introduced for loop antennas. Based on the loop antenna in Fig. 1, a grounding strip is placed near the feeding point as shown in Fig. 5(a). This parasitic element can create one mode to cover LTE band 42 (3400–3600 MHz), which can be seen from Fig. 5(b).

However, this technique cannot be used to excite a mode in 5-GHz band for LTE-U/LTE-LAA through our simulation. In order to explain the reason, the vector current distribution at 5.5 GHz is shown in Fig. 5(c) for LL = 8.5 mm. From Fig. 5(c), it can be observed that there are two antiphase currents that simultaneously couple electromagnetic field energy from the main loop antenna to the single-mode parasitic element. Nevertheless, the coupling energy from the two antiphase currents excites the same 0.25λ modes but with antiphase, so the excited 0.25λ modes will cancel each other. As a result, the single-mode parasitic element cannot be excited efficiently in 5-GHz band.

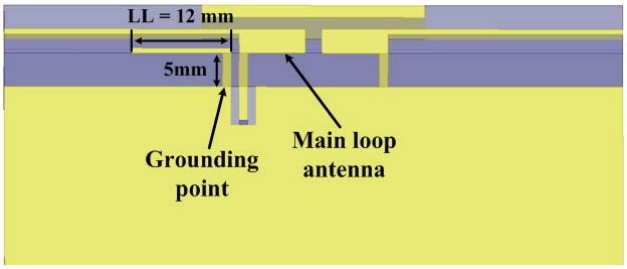

(a)

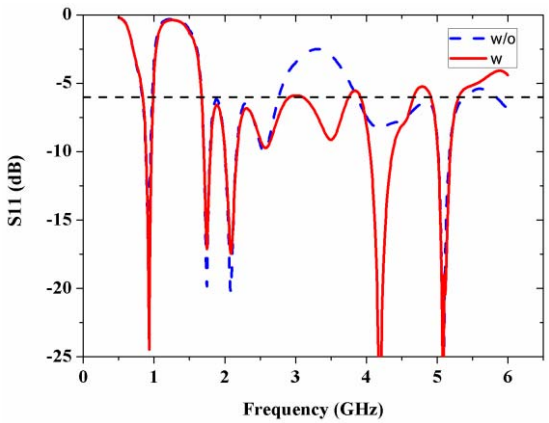

(b)

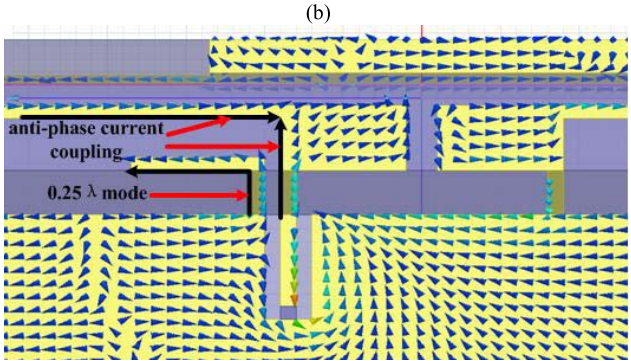

(c)

Fig. 5. (a) Configuration of single-mode parasitic element. (b) Comparison of $S11$ between loop antennas with and without single-mode parasitic element. (c) Vector current distribution at 5.5 GHz when LL = 8.5 mm.

2) Monopole/Dipole Parasitic Element: To solve the energy cancellation problem, an abstract current path model is extracted from Fig. 5(c) and shown in Fig. 6(a). I_{loop1} and I_{loop2} are the corresponding antiphase currents on the main loop antenna; I_{pe} is the excited mode current on the parasitic element; α is the coupling coefficient between I_{loop1} and I_{pe}, and β is the coupling coefficient between I_{loop2} and I_{pe}; and α and β are always positive. In type I, which is the case of the single-mode parasitic element, I_{loop1} provides a positive coupling to I_{pe}, while I_{loop2} provides a negative coupling to I_{pe}, so I_{pe} can be written as

$$I_{\text{pe}} = \alpha I_{\text{loop1}} - \beta I_{\text{loop2}}. \quad (1)$$

From the equation, if we want to avoid the negative coupling, β should be equal to zero. Therefore, part of the current path that is parallel to I_{loop2} is removed in type II. Then, I_{pe} can be written as

$$I_{\text{pe}} = \alpha I_{\text{loop1}}. \quad (2)$$

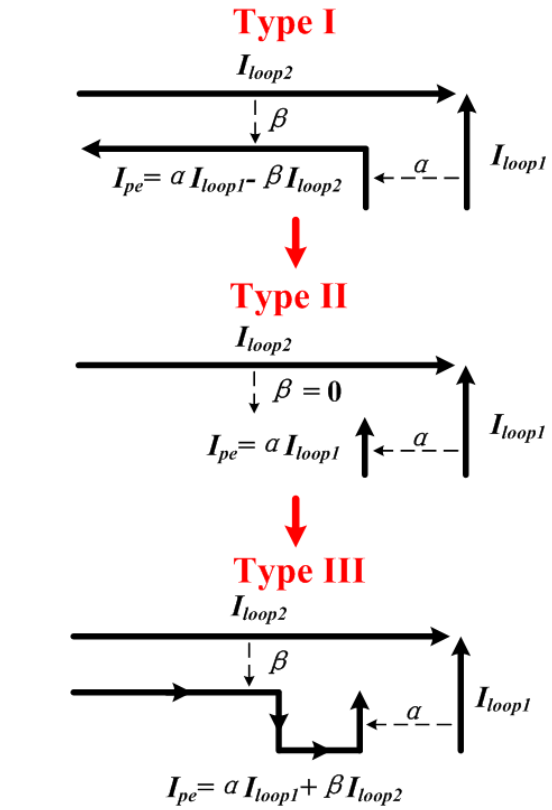

(a)

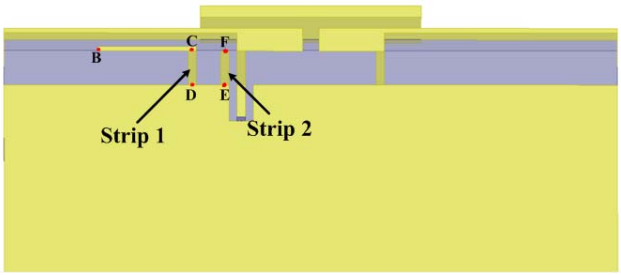

(b)

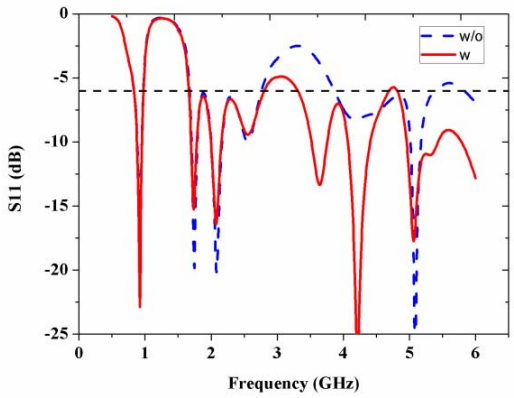

(c)

Fig. 6. (a) Current path model for the evolution of parasitic element technology. (b) Configuration of monopole/dipole parasitic element. BC = 12 mm, CD = 5 mm, DE = 4 mm, and FE = 5 mm. (c) Comparison of $S11$ between loop antennas with and without monopole/dipole parasitic element.

However, in this case, the physical length of the corresponding parasitic element can be 5 mm at the maximum because of the thickness limit of smartphones; it is too short for the

parasitic element to resonate in 5-GHz band. Thus, we need to create a new current path for the parasitic element to extend its electrical length; besides, the new path should be able to avoid the negative coupling and even obtain more positive coupling from I_{loop1} and I_{loop2}. One effective solution is shown in type III. From the current distribution in type III, it can be seen that although I_{loop1} and I_{loop2} are antiphase, they both provide positive coupling to the new current path. As a result, I_{pe} can be written as

$$I_{\text{pe}} = \alpha I_{\text{loop1}} + \beta I_{\text{loop2}}. \tag{3}$$

By removing part of the old current path and creating a new current path, the minus in (1) has been successfully converted into a plus in (3); this means more efficient excitation for the parasitic element mode. The next step is to realize the current path of type III in actual antenna structure.

Based on the loop antenna in Fig. 1, two grounding strips are placed near the feeding point as shown in Fig. 6(b). Strip 2 itself is corresponding to the current path I_{pe} in type II, but it is too short to resonate in 5-GHz band (it should resonate at around 15 GHz as a monopole parasitic element), so strip 1 together with the ground is used to create a dipole current path for strip 2; this dipole current path is corresponding to the current path I_{pe} in type III. In other words, section BCDEF is a dipole parasitic element. Besides, it is easy to find that section BCD can also operate as a monopole parasitic element. As a result, the proposed parasitic element can operate at a monopole-like 0.25λ mode and a dipole-like 0.5λ mode simultaneously.

As discussed above, the resonant frequency of monopole-like 0.25λ mode is determined by the length of section BCD, while the resonant frequency of dipole-like 0.5λ mode is determined by the length of section BCDEF. Therefore, these two modes can be tuned separately. In this design, the monopole-like 0.25λ mode is used to cover 3400–3800 MHz for LTE bands 42/43, and the dipole-like 0.5λ mode in conjunction with other higher order modes of the loop antenna is used to cover 5150–5850MHz for LTE-U/LTE-LAA as shown in Fig. 6(c). From Fig. 6(c), it is also notable that the proposed monopole/dipole parasitic element has little effect on the main loop antenna modes, which makes it easy to design.

C. Radiation Mechanisms

In order to further demonstrate the principle of the proposed antenna, surface current distributions and 3-D radiation patterns of six resonant modes are simulated and shown in Figs. 7 and 8, respectively. From the $S11$ in Fig. 6(c), it can be easily seen that 0.5λ, 1λ, 1.5λ, 2λ, monopole-like 0.25λ, and dipole-like 0.5λ modes resonate at around 920, 1745, 2085, 2560, 3640, and 5345 MHz, respectively. Therefore, these frequency points are chosen for the demonstration.

From vector surface current distributions in Fig. 7(a)–(d), it is clearly shown that there are one, two, three, and four current nulls on loop antenna track, respectively. This proves that these four modes are 0.5λ, 1λ, 1.5λ, and 2λ modes, respectively. From vector surface current distribution in Fig. 7(e), it can be observed that there is strong current on strip 1,

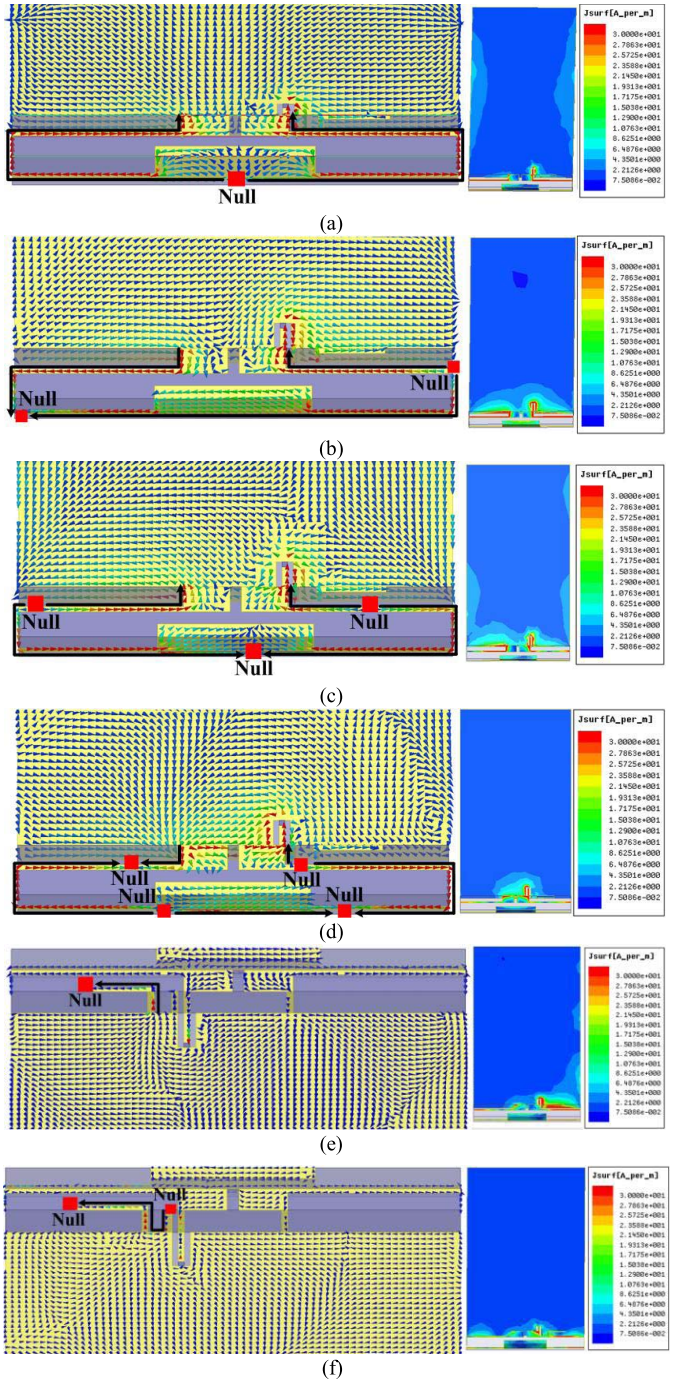

Fig. 7. Vector surface current distributions and current density distributions at (a) $f = 920$ MHz, (b) $f = 1745$ MHz, (c) $f = 2085$ MHz, (d) $f = 2560$ MHz, (e) $f = 3640$ MHz, and (f) $f = 5345$ MHz.

and only one current null exists at the open end of strip 1 together with one current maximum at the grounding point of strip 1, so this mode is monopole-like 0.25λ mode that is an unbalanced mode. Besides, there is little energy on strip 2 in this case, so strip 2 does not work at this mode. From vector surface current distribution in Fig. 7(f), it is easy to find that there is strong current along the path from strip 1 to strip 2, and there are one current null at the open end of strip 1, another current null at the open end of strip 2, and

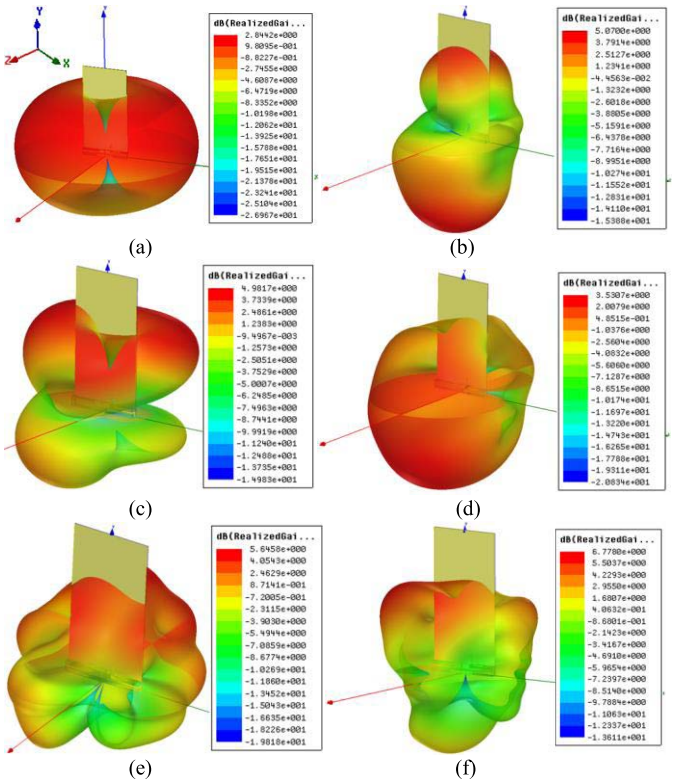

Fig. 8. Simulated 3-D radiation patterns at (a) $f = 920$ MHz, (b) $f = 1745$ MHz, (c) $f = 2085$ MHz, (d) $f = 2560$ MHz, (e) $f = 3640$ MHz, and (f) $f = 5345$ MHz.

one current maximum in the middle of the path. As a result, this mode is dipole-like 0.5λ mode, which is a balanced mode.

Balanced modes are superior to unbalanced modes because there is much less current density distribution on PCB, which benefits user interaction robustness. From the surface current density distributions in Fig. 7(a)–(f), it can be clearly seen that for the current distribution on PCB, the energy of 1λ, 2λ, and dipole-like 0.5λ modes is much weaker than the energy of 0.5λ, 1.5λ, and monopole-like 0.25λ modes. This phenomenon also demonstrates that the first introduced dipole-like 0.5λ mode for parasitic element is a balanced mode from another point of view.

From the 3-D radiation patterns shown in Fig. 8(a)–(d), it can be observed that these four 3-D patterns are typical patterns of loop antenna 0.5λ, 1λ, 1.5λ, and 2λ modes, respectively. The pattern in Fig. 8(e) has more nulls than the patterns in Fig. 8(a)–(d), because the radiator of this mode, which consists of strip 1 and PCB, has much larger electrical size. It can also be seen that most of electromagnetic field energy radiates toward the $+y$ direction. It is because the radiated energy from the source current of strip 1 and the induced current on PCB will in-phase stack, but PCB exists only in the $+y$ direction, so the induced current exists only in the $+y$ direction but not in the $-y$ direction, and thus the phenomenon of in-phase stacking happens only in the $+y$ direction but not in the $-y$ direction. From Fig. 8(f), it can be found that most of the energy radiates along the y-axis. The reason is that the main radiation source of this mode is strip 1 and strip 2, so the current concentrates on these two strips, which means the current direction is along either the x-axis or the z-axis and the current in both directions has the strongest radiation in the y-direction.

D. Design Guidance

In general, the design of multimode antennas is complicated because designers need to take into account all the operating modes simultaneously. In order to simplify the design complexity of the proposed six-mode antenna, some design principles are given as follows.

1) The six-mode design can be divided into two parts, i.e., the design of the four loop antennas modes and the design of the two parasitic element modes. As shown in Fig. 6(c), the parasitic element modes have little effect on the operating state of the loop antenna modes. As a result, designers can design the main loop antenna first and add the monopole/dipole parasitic element afterward. Four-mode design and two-mode design should be much easier than the six-mode design.
2) For the loop antenna design, the initial length of the loop antenna should be set as half-wavelength at 900 MHz. That is

$$2 \times (2 \times H + L1 + L2 + L3) + L = \lambda_1/2 \quad (4)$$

$$\lambda_1 = c/f_1 \quad (5)$$

where c is the speed of light in vacuum and f_1 is the frequency value of 900 MHz. Then, the widened portion A should be added and maintained during the whole tuning process. Afterward, utilize reactive loading (in the proposed antenna, it is the widened portion with a width of $H + L5$) to tune the resonant frequency of 0.5λ, 1λ, 1.5λ, and 2λ modes to proper position. Finally, a high-pass matching circuit should be used to expand the bandwidth of 0.5λ mode.
3) For the design of the monopole/dipole parasitic element, the initial length of the monopole path and the dipole path should be set as quarter-wavelength at 3600 MHz and half-wavelength at 5500 MHz, respectively. That is

$$BC + CD = \lambda_2/4 \quad (6)$$

$$BC + CD + DE + EF = \lambda_3/2 \quad (7)$$

$$\lambda_2 = c/f_2 \quad (8)$$

$$\lambda_3 = c/f_3 \quad (9)$$

where f_2 is the frequency value of 3600 MHz and f_3 is the frequency value of 5500 MHz. However, the resonant frequency of the monopole-like 0.25λ mode and the dipole-like 0.5λ mode may deviate from 3600 and 5500 MHz due to the complex electromagnetic coupling environment. Further fine tuning is needed.

III. Measured Results and Discussion

The proposed antenna has been fabricated and measured, and the prototype is shown in Fig. 9(a). As shown in Fig. 9(b), a high-pass network, which consists of one shunt inductor

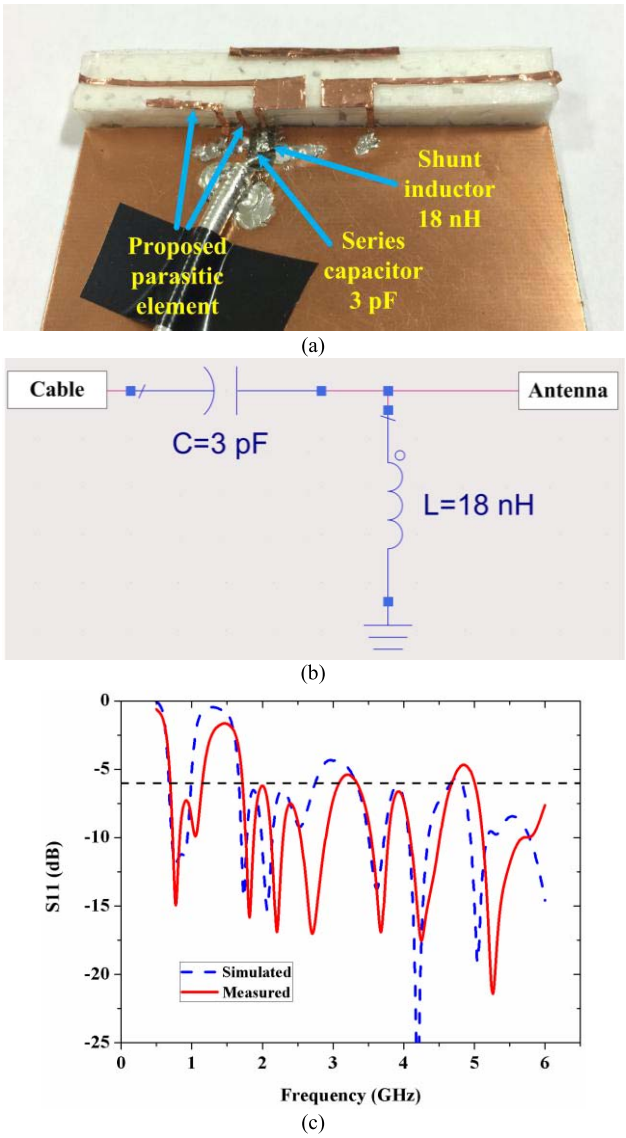

Fig. 9. (a) Fabricated antenna. (b) High-pass matching circuit. (c) Simulated and measured $S11$ of the proposed antenna.

($L = 18$ nH) and one series capacitor ($C = 3$ pF), is adopted to enhance the bandwidth of 0.5λ mode and have little influence on the frequency bands above 1.5 GHz. The simulated $S11$ of the antenna with the matching circuit is shown in Fig. 9(c). From the measured $S11$ in Fig. 9(c), it can be seen that the four loop antenna modes and the two proposed parasitic element modes have been successfully excited to cover the bands of 660–1100, 1710–3020, 3370–3900, and 5150–5850 MHz, which is wide enough for almost all the service of mobile telecommunication systems. In the measured result, the resonant frequency of the six modes is a little higher than the simulated result because of the rough handmade prototype. However, it still indicates good agreement between the measured and simulated results.

The simulated and measured radiation efficiency is shown in Fig. 10. In the bands of 690–1100 and 1710–3020 MHz, the frequency of peak points in the measured efficiency is also higher than that in the simulated efficiency because of the fabrication error. In the band of 3370–3900 MHz, the

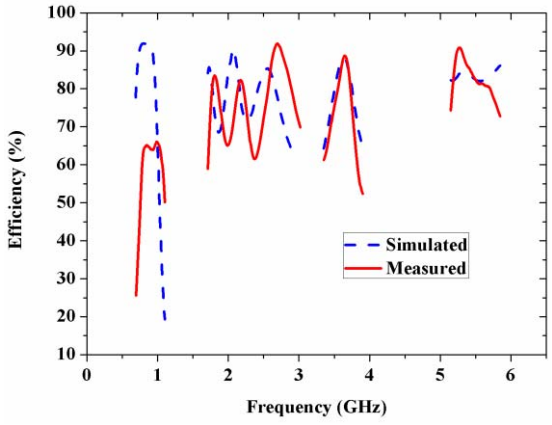

Fig. 10. Simulated and measured radiation efficiency.

TABLE I
BANDWIDTH COMPARISON

Ref.	Proposed	[4]	[5]	[7]	[8]
Clearance area (mm^2)	75×10	50×13	68×3	60×8	70×10 +70×5
-6 dB bandwidth (MHz)	660-1100 1710-3020 3370-3900 5150-5850	698-960 1710-2300 — —	780-1020 1650-2120 — —	800-1100 1700-2580 — —	770-1130 1612-3000 — —
>59% efficiency bandwidth (MHz)	775-1070 1710-3020 3370-3840 5150-5850	720-960 1710-2300 — —	820-1000 — — —	830-1140 1680-2570 — —	824-960 1710-2690 — —

measured result shows excellent agreement with the simulated result. In the band of 5150–5850 MHz, the measured curve is a little different from the simulated curve because the electrical characteristics are much more sensitive in such a high frequency, which means that small dimension error may cause big difference. It should be noted that the measured efficiency at around 2.7 and 5.27 GHz is higher than the simulated result. The reason is that at 2.7 and 5.27 GHz, the measured $S11$ [shown in Fig. 9(c)] is much better than the simulated $S11$, so the total radiation percentage of electromagnetic field energy increases a lot. In summary, reasonable agreement is obtained between the measured and simulated results.

The bandwidth of the measured radiation efficiency better than 30% is 704–1100, 1710–3020, 3370–3840, and 5150–5850 MHz. If efficiency better than 59% is chosen as the criteria, the bandwidth should be 775–1070, 1710–3020, 3370–3840, and 5150–5850 MHz. It should be mentioned that in practical applications, the 0.5λ mode of the loop antenna can be tuned to lower resonant frequency to achieve better efficiency in the band of 698–960 MHz.

IV. CONCLUSION

A novel multiband loop antenna with six resonant modes has been proposed for LTE smartphones. The distinctive feature of the proposed antenna is that the proposed monopole/dipole parasitic element offers one extra monopole-like 0.25λ mode and one extra balanced dipole-like 0.5λ mode, which together with four loop antenna modes can be utilized

to cover the bands of 660–1100, 1710–3020, 3370–3900, and 5150–5850 MHz. These four bands are wide enough for almost all the service of mobile telecommunication systems such as GSM850, GSM900, DCS1800, PCS1900, UMTS, 2.4-GHz Wi-Fi, FDD-LTE bands (1-10, 12-14, 17-20, 22, 23, 25-31), TDD-LTE bands (33-44), and even the coming LTE-U/LTE-LAA. Bandwidth comparison between our proposed loop antenna and the loop antennas in the latest published papers is shown in Table I. It can be clearly seen that the proposed antenna has the widest bandwidth in an acceptable clearance area.

Another advantage of the proposed antenna is the extra balanced mode, i.e., dipole-like 0.5λ mode of the parasitic element. It should be the first time to report a balanced mode for a parasitic element. Furthermore, the proposed antenna should be the first loop antenna that has three balanced modes. As is known, balanced modes have better user interaction robustness and smaller specific absorption rate than unbalanced modes. This enables the proposed antenna to provide better user experience. It is also worth mentioning that the proposed monopole/dipole parasitic element does not need any additional space for loop antennas and has little effect on the main loop antenna modes. This makes the parasitic element easy to design and tune in practical applications. Some design principles have been given in this paper.

Overall, the proposed antenna has solved the problem of excellent user experience but limited bandwidth in loop antennas. It is a promising candidate for LTE smartphone application.

ACKNOWLEDGMENT

The authors would like to thank S. Jakes from the University of Kent for the antenna fabrication. They would also like to thank S. Ariffin from the University of Kent for her help in English writing.

REFERENCES

[1] Y. W. Chi and K. L. Wong, "Compact multiband folded loop chip antenna for small-size mobile phone," *IEEE Trans. Antennas Propag.*, vol. 56, no. 12, pp. 3797–3803, Dec. 2008.

[2] K. L. Wong and C. H. Huang, "Printed loop antenna with a perpendicular feed for penta-band mobile phone application," *IEEE Trans. Antennas Propag.*, vol. 56, no. 7, pp. 2138–2141, Jul. 2008.

[3] H. F. Abutarboush *et al.*, "Multiband inverted-F antenna with independent bands for small and slim cellular mobile handsets," *IEEE Trans. Antennas Propag.*, vol. 59, no. 7, pp. 2636–2645, Jul. 2011.

[4] M. Zheng, H. Wang, and Y. Hao, "Internal hexa-band folded monopole/dipole/loop antenna with four resonances for mobile device," *IEEE Trans. Antennas Propag.*, vol. 60, no. 6, pp. 2880–2885, Jun. 2012.

[5] K. Ishimiya, C.-Y. Chiu, and J.-I. Takada, "Multiband loop handset antenna with less ground clearance," *IEEE Antennas Wireless Propag. Lett.*, vol. 12, pp. 1444–1447, 2013.

[6] K.-L. Wong and M.-T. Chen, "Small-size LTE/WWAN printed loop antenna with an inductively coupled branch strip for bandwidth enhancement in the tablet computer," *IEEE Trans. Antennas Propag.*, vol. 61, no. 12, pp. 6144–6151, Dec. 2013.

[7] D. Wu, S. W. Cheung, and T. I. Yuk, "A compact and low-profile loop antenna with multiband operation for ultra-thin smartphones," *IEEE Trans. Antennas Propag.*, vol. 63, no. 6, pp. 2745–2750, Jun. 2015.

[8] Y.-L. Ban, Y.-F. Qiang, Z. Chen. K. Kang, and J.-H. Guo, "A dual-loop antenna design for hepta-band WWAN/LTE metal-rimmed smartphone applications," *IEEE Trans. Antennas Propag.*, vol. 63, no. 1, pp. 48–58, Jan. 2015.

[9] M. Zheng, "Multi-band antenna," U.S. Patent 7 307 591 B2, Dec. 11, 2004.

[10] H. Y. Wang, M. Zheng, and S. Brett, "Multi-band antenna arrangement," U.S. Patent 7 205 942 B2, Apr. 17, 2007.

[11] Y. Li, Z. Zhang, J. Zheng, Z. Feng, and M. F. Iskander, "A compact hepta-band loop-inverted F reconfigurable antenna for mobile phone," *IEEE Trans. Antennas Propag.*, vol. 60, no. 1, pp. 389–392, Jan. 2012.

[12] Y. Li, Z. Zhang, J. Zheng, and Z. Feng, "Compact heptaband reconfigurable loop antenna for mobile handset," *IEEE Antennas Wireless Propag. Lett.*, vol. 10, pp. 1162–1165, 2011.

[13] H.-T. Chen, K.-L. Wong, and T.-W. Chiou, "PIFA with a meandered and folded patch for the dual-band mobile phone application," *IEEE Trans. Antennas Propag.*, vol. 51, no. 9, pp. 2468–2471, Sep. 2003.

[14] H. Wang and M. Zheng, "An internal triple-band WLAN antenna," *IEEE Antennas Wireless Propag. Lett.*, vol. 10, pp. 569–572, 2011.

[15] K.-L. Wong, W.-Y. Chen, and T.-W. Kang, "On-board printed coupled-fed loop antenna in close proximity to the surrounding ground plane for penta-band WWAN mobile phone," *IEEE Trans. Antennas Propag.*, vol. 59, no. 3, pp. 751–757, Mar. 2011.

[16] Y.-L. Ban, C.-L. Liu, J. L.-W. Li, J. Guo, and Y. Kang, "Small-size coupled-fed antenna with two printed distributed inductors for seven-band WWAN/LTE mobile handset," *IEEE Trans. Antennas Propag.*, vol. 61, no. 11, pp. 5780–5784, Nov. 2013.

[17] L. Li, Z. Jia, F. Huo, and W. Han, "A novel compact multiband antenna employing dual-band CRLH-TL for smart mobile phone application," *IEEE Antennas Wireless Propag. Lett.*, vol. 12, pp. 1688–1691, 2013.

[18] H. Liu, B. Lu, and L. Li, "Novel miniaturized octaband antenna for LTE smart handset applications," *Int. J. Antennas Propag.*, vol. 2015, Art. no. 861016. [Online]. Available: http://www.hindawi.com/journals/ijap/2015/861016/

[19] Y.-W. Chi and K.-L. Wong, "Internal compact dual-band printed loop antenna for mobile phone application," *IEEE Trans. Antennas Propag.*, vol. 55, no. 5, pp. 1457–1462, May 2007.

[20] C.-I. Lin and K.-L. Wong, "Internal meandered loop antenna for GSM/DCS/PCS multiband operation in a mobile phone with the user's hand," *Microw. Opt. Technol. Lett.*, vol. 49, pp. 759–766, Apr. 2007.

[21] H. Morishita, H. Furuuchi, and K. Fujimoto, "Performance of balance-fed antenna system for handsets in the vicinity of a human head or hand," *IEE Proc.-Microw. Antennas Propag.*, vol. 149, no. 2, pp. 85–91, Apr. 2002.

[22] Qualcomm. (Sep. 2015). *Making the Best Use of Licensed and Unlicensed Spectrum*. https://www.qualcomm.com/media/documents/files/making-the-best-use-of-unlicensed-spectrum-presentation.pdf

[23] R. Zhang, M. Wang, L. X. Cai, Z. Zheng, X. Shen, and L.-L. Xie, "LTE-unlicensed: The future of spectrum aggregation for cellular networks," *IEEE Wireless Commun.*, vol. 22, no. 3, pp. 150–159, Jun. 2015.

[24] ANSYS/ANSOFT. (2012). *High Frequency Structure Simulator (HFSS) ver. 13.0*. [Online]. Available: http://www.ansoft.com/products/hf/hfss/

[25] *Testing and Measurement Techniques-Reverberation Chamber Test Methods*, document IEC 61000-4-21, 2011.

[26] C. L. Holloway, H. A. Shah, R. J. Pirkl, W. F. Young, D. A. Hill, and J. Ladbury, "Reverberation chamber techniques for determining the radiation and total efficiency of antennas," *IEEE Trans. Antennas Propag.*, vol. 60, no. 4, pp. 1758–1770, Apr. 2012.

[27] Q. Xu, Y. Huang, X. Zhu, L. Xing, Z. Tian, and C. Song, "A modified two-antenna method to measure the radiation efficiency of antennas in a reverberation chamber," *IEEE Antennas Wireless Propag. Lett.*, vol. 15, pp. 336–339, 2016.

[28] H. Wang and M. Zheng, "Triple-band wireless local area network monopole antenna," *IET Microw. Antennas Propag.*, vol. 2, no. 4, pp. 367–372, Jun. 2008.

[29] P. Vainikainen, J. Ollikainen, O. Kivekas, and I. Kelander, "Resonator-based analysis of the combination of mobile handset antenna and chassis," *IEEE Trans. Antennas Propag.*, vol. 50, no. 10, pp. 1433–1444, Oct. 2002.

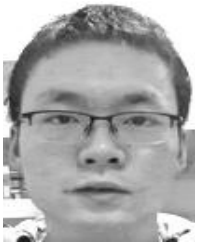

Hang Xu received the B.S. and M.S. degrees from the University of Electronic Science and Technology of China, Chengdu, China, in 2009 and 2013, respectively. He is currently pursuing the Ph.D. degree with the University of Kent, Canterbury, U.K.

His current research interests include 5G smartphone antennas, MIMO antenna arrays, decoupling technology, and microwave and millimeter-wave antennas.

Hanyang Wang (SM'03) received the Ph.D. degree from Heriot-Watt University, Edinburgh, U.K., in 1995.

He served as a Lecturer and an Associate Professor with Shandong University, Jinan, China, from 1986 to 1991. From 1995 to 1999, he was a Post-Doctoral Research Fellow with the University of Birmingham, Birmingham, U.K., and the University of Essex, Colchester, U.K. From 1999 to 2000, he was with Vector Fields Ltd., Oxford, U.K., as a Software Development and Microwave Engineering Consultant Engineer. He joined Nokia U.K. Ltd., Dartford, U.K., in 2001, where he was a Mobile Antenna Specialist for 11 years. He joined Huawei Technologies Company, Ltd., Reading, U.K., after leaving Nokia, and he is currently the Chief Antenna Expert and the Head of the Mobile Antenna Technology Division. He is also an Adjunct Professor with the School of Electronics and Information Technology, Sichuan University, Chengdu, China. He holds over 20 granted and pending U.S. or WO patents. He has authored over 70 refereed papers on these topics. His current research interests include small antennas for mobile terminals, patch and slotted waveguide antennas and arrays for mobile communications and airborne radars, and numerical methods for the solutions of electromagnetic radiation and scattering problems.

Dr. Wang is an IET/IEE Fellow and a Huawei Fellow. He was a recipient of the Title of Nokia Inventor of the Year in 2005 and the Nokia Excellence Award in 2011. He was also a recipient of the Huawei Individual Gold Medal Award in 2012 and the Huawei Team Gold Medal Award in 2013 and 2014, respectively. He is an Associate Editor of the *IEEE Antennas and Wireless Propagation Letters*. He is listed in *Marquis Who's Who in the World* and the International Biographical Center, Cambridge, U.K.

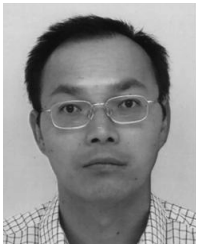

Steven Gao (M'01) received the Ph.D. degree in microwave engineering from Shanghai University, Shanghai, China.

He started his career in 1994 while with the China Research Institute of Radiowave Propagation, Xinxiang, China. Afterward, he was a Postdoctoral Research Fellow with the National University of Singapore, Singapore, a Research Fellow with Birmingham University, Birmingham, U.K., a Visiting Research Scientist with the Swiss Federal Institute of Technology, Zürich, Switzerland, a Visiting Fellow with Chiba University, Chiba, Japan, a Visiting Scientist with the University of California at Santa Barbara, Santa Barbara, CA, USA, a Senior Lecturer, a Reader, and the Head of the Antenna and Microwave Group with Northumbria University, Newcastle upon Tyne, U.K., and the Head of the Satellite Antennas and RF System Group with the Surrey Space Center, University of Surrey, Surrey, U.K. Since January 2013, he has been a Professor with the University of Kent, Canterbury, U.K., where he is currently the Chair of RF and Microwave Engineering. He co-edited the book entitled *Space Antenna Handbook* (Wiley, 2012), and co-authored the book entitled *Circularly Polarized Antennas* (IEEE-Wiley, 2014), over 250 papers, and several patents. His current research interests include smart antennas, phased arrays, MIMO, satellite antennas, microwave/millimeter-wave/THz circuits, satellite and mobile communications, and radar (UWB radar and synthetic-aperture radar) and wireless power transfer.

Dr. Gao is a Fellow of IET. He is an IEEE AP-S Distinguished Lecturer, an Associate Editor of the IEEE TRANSACTIONS ON ANTENNAS AND PROPAGATION and *Radio Science*, and the Editor-in-Chief of the *Microwave and Wireless Technologies* (Wiley Book Series). He was the General Chair of LAPC 2013, and an Invited or Keynote Speaker at international conferences such as AES'2014, IWAT'2014, SOMIRES'2013, and APCAP'2014.

Hai Zhou received the Ph.D. degree in reflector antenna synthesis from the University of London, London, U.K., in 1987.

He carried out his Postdoctoral work with the University of London until 1992. He served as a Senior Lecturer with South Bank University, London. He joined Lucent Technologies, Murray Hill, NJ, USA, in 1996, where he was involved in GSM, UMTS, and LTE in system engineering. He joined Huawei Technologies Company, Ltd., Reading, U.K., in 2015. He worked on various topics such as shaped reflector antenna synthesis, FDTD, and radio resource management and adaptive antennas in the industry. He holds 18 patents, and has published 14 journal papers and 34 conference papers.

Dr. Zhou received a Best Paper Award at the 19th European Microwave Conference in 1989 and the Oliver Lodge premium from the Institution of Electrical Engineers for the Best Paper of the Year on Antennas and Propagation in 1991.

Yi Huang (S'91–M'96–SM'06) is a Chair Professor of Wireless Engineering, University of Liverpool, U.K. He has published over 300 refereed papers in journals and conference proceedings, two books on antennas and EMC, and has served on many national and international technical committees.

Prof. Huang is a Fellow of the IET.

Qian Xu received the Ph.D. degree in electrical engineering from the University of Liverpool, Liverpool, U.K., in 2016.

Yujian Cheng (SM'14) is currently a Professor with the University of Electronic Science and Technology of China, Chengdu, China.